The Desmoplakin Carboxyl Terminus Coaligns with and Specifically Disrupts Intermediate Filament Networks When Expressed in Cultured Cells

Thaddeus S. Stappenbeck and Kathleen J. Green

Department of Pathology and the Cancer Center, Northwestern University Medical School, Chicago, Illinois 60611

Abstract. Specific interactions between desmoplakins I and II (DP I and II) and other desmosomal or cytoskeletal molecules have been difficult to determine in part because of the complexity and insolubility of the desmosome and its constituents. We have used a molecular genetic approach to investigate the role that DP I and II may play in the association of the desmosomal plaque with cytoplasmic intermediate filaments (IF). A series of mammalian expression vectors encoding specific predicted domains of DP I were transiently expressed in cultured cells that form (COS-7) and do not form (NIH-3T3) desmosomes. Sequence encoding a small antigenic peptide was added to the 3′ end of each mutant DP cDNA to facilitate immunolocalization of mutant DP protein. Light and electron microscopical observations revealed that DP polypeptides including the 90-kD carboxy-terminal globular domain of DP I specifically colocalized with and ultimately resulted in the complete disruption of IF in both cell lines. This effect was specific for IF as microtubule and microfilament networks were unaltered. This effect was also specific for the carboxyl terminus of DP, as the expression of the 95-kD rod domain of DP I did not visibly alter IF networks. Immunogold localization of COS-7 cells transfected with constructs including the carboxyl terminus of DP demonstrated an accumulation of mutant protein in perinuclear aggregates within which IF subunits were sequestered. These results suggest a role for the DP carboxyl terminus in the attachment of IF to the desmosome in either a direct or indirect manner.

Desmosomes are intercellular junctions that function in cell–cell adhesion and act as specific cell surface attachment sites for intermediate filaments (IF)[1] (for reviews see Steinberg et al., 1987; Garrod et al., 1990; Green and Jones, 1990; Schwarz et al., 1990). The supracellular network of cytoplasmic IF and desmosomes is found in a number of tissues such as epithelia, myocardium, and arachnoid where desmosomes interact with keratin, desmin, and vimentin IF, respectively (Schwarz et al., 1990). While the exact function of IF has yet to be fully understood (Steinert and Roop, 1988; Klymkowsky et al., 1989), the ultrastructure of the IF–desmosome network suggests that in addition to maintaining the integrity and proper relationship among cells, it may impart increased tensile strength and mechanical resistance to whole tissues (Arnn and Staehelin, 1981). Recent work that supports this idea demonstrated that transgenic mice with disrupted IF in the basal layer of stratified epithelia displayed abnormalities in epidermal architecture and blistered easily (Vasser et al., 1991). Although cytoplasmic IF have been extensively investigated, the exact nature and importance of the link to desmosomes is unknown.

1. *Abbreviations used in this paper*: DP, desmoplakins; IF, intermediate filaments; PCR, polymerase chain reaction.

Ultrastructurally, desmosomes appear as disc-shaped regions, 0.5–2.0 μm in diameter and ~100-nm thick, symmetrically arranged about two adjacent cell membranes. Between the plasma membranes is a 20–30-nm space which contains the extracellular domains of the transmembrane glycoproteins of the desmosome (or desmoglea). The cytoplasmic portion of the desmosome consists of an electron-dense, trilaminar plaque of variable thickness (10–40 nm), which underlies both cell membranes (Schwarz et al., 1990). IF are thought to interact with the desmosome by looping through the innermost plaque region (Kelly, 1966).

The highly related molecules, desmoplakins I and II (DP I and II), are the most abundant constituents of the cytoplasmic plaque region of the desmosome (Mueller and Franke, 1983; Kapprell et al., 1985). Based on an analysis of the predicted amino acid sequence (Green et al., 1990), DP I is predicted to form a homodimer comprising a central α-helical coiled-coil dimer ~130-nm long, flanked by two globular ends corresponding to the amino and carboxy termini of the molecule. This prediction is consistent with the biochemical evidence that purified and crosslinked DP I exists as a dimer in vitro. Furthermore, rotary shadowed images of purified DP I (O'Keefe et al., 1989) appeared dumbbell shaped with a central "rod" of the length predicted by Green

et al. (1990). The rod domain of DP I is characteristic of many α-fibrous proteins including IF in that it is predominantly composed of a series of heptad repeats (Conway and Parry, 1990). DP II is thought to be derived from an alternatively spliced mRNA of DP I resulting in a greatly shortened rod domain (Green et al., 1990).

One particularly interesting feature of the 851 amino acid carboxyl terminus of DP I and II is a series of three regions that contain 4.6 copies of a 38-residue repeat (Green et al., 1990). The periodicity of the acidic and basic residues of these repeats matches that of the 1B rod domain of IF thus indicating a basis for potential ionic interaction between the two molecules. The possibility that DP links IF to the desmosome has been previously suggested based on a number of observations (Green and Jones, 1990). Furthermore, the 38-residue repeat has also been found in the carboxyl terminus of plectin, which is a known IF-associated protein (Wiche et al., 1991), and the 230-kD bullous pemphigoid antigen (Green et al., 1990; Tanaka et al., 1991), which has been localized to the plaque region of hemidesmosomes. Hemidesmosomes act as attachment sites for IF at the dermal-epidermal junction (Green and Jones, 1990), so it is intriguing that this junction contains a plaque component similar to DP in desmosomes.

One difficulty with the proposed DP-mediated linkage of IF to the desmosome is that previous attempts using biochemical techniques have been unable to demonstrate an interaction between DP and IF or any other molecule (O'Keefe et al., 1989; Pasdar et al., 1991). There are several possible explanations for these results. First, if DP does directly bind IF, it is possible that the denaturing conditions used to extract DP from desmosomes during purification affected the in vitro binding capacity of DP. Another possibility is that DP may interact directly with IF, but only in the presence of accessory proteins that would stabilize the interaction. A third possibility is that one or more linking proteins mediate an indirect association of DP and IF. The possibilities that accessory or linking proteins may be involved must be considered as the desmosomal plaque is complex and a number of other desmosomal molecules have been proposed as IF linkers (Tsukita and Tsukita, 1985; Kapprell et al., 1988; Cartaud et al., 1990; Foisner et al., 1991). To avoid difficulties inherent with in vitro binding experiments, we have chosen a molecular genetic approach to test the possible interaction between the carboxyl terminus of DP and IF in cells that would contain any putative cofactors or linking proteins. Using the previously characterized partial cDNA of DP I, the carboxyl terminus with and without the rod domain of DP I was expressed in tissue culture cells. By tracking the pattern of expression of mutant protein by immunofluorescence and immunogold EM, we found that the carboxyl terminus of DP specifically coaligned with and eventually resulted in the disruption of IF networks.

Materials and Methods

Cell Culture

COS-7 African Green monkey kidney cells that constitutively express SV-40 large T antigen, thus replicating plasmids with an SV-40 origin of replication to a high number (Gluzman, 1981) and NIH-3T3 mouse fibroblasts were cultured in DME plus 10% FCS and 100 U/ml penicillin and 100 μg/ml streptomycin.

Construction of Expression Vectors

For each construct, polymerase chain reaction (PCR) mutagenesis was performed to generate sequence for a molecular tag, an artificial start, and a stop site. AmpliTaq DNA polymerase (Perkin-Elmer Corp., Norwalk, CT) was used according to the manufacturer's instructions in a reaction with 10 ng of the appropriate DP I cDNA and 1 μM of the appropriate oligos. After PCR amplification for 35 cycles (1 min at 94°C, 2 min at 45°C for cycles 1–5, and 2 min at 55°C for cycles 6–35, 1 min at 72°C), products were isolated from a polyacrylamide gel, subcloned into pGEM-9Zf(−) (Promega Corp., Madison, WI) and sequenced using the Sequenase Kit (United States Biochemical, Cleveland, OH) to confirm that the correct sequences had been inserted.

Construction of pDP.CT. A 34-mer oligonucleotide 5′-AAGAGCTCGCCATGGgagcatctgcttctccta-3′ (Northwestern Biotechnology Research Service Facilities, Chicago, IL) was used to insert sequence encoding a SacI restriction site followed by a portion of the Kozak (Kozak, 1986) consensus sequence for ribosome binding and an ATG start site (both underlined) 5′ of the predicted carboxyl terminus (lower case). This oligo in the sense orientation was used in a PCR reaction with an antisense oligo 5′-CTGTCGACAGTCAGCTT-3′ that was located at an internal SalI site 150-bp downstream from the start site of the carboxyl terminus. This 150-bp SacI/SalI fragment was subcloned into a plasmid containing a 2.4-kb SalI/EcoRI fragment of DP cDNA encoding a major portion of the carboxyl terminus (pl). A 71-mer oligo 5′-agcagtagttctattgggcacGTGGAGCAAAAGCTCATTTCTGAAGAGGACTTGTAGGGTACCGAATTCCC-3′ was used to insert sequence encoding a 33-bp *c-myc* epitope (underlined), a stop codon and a KpnI and an EcoRI restriction site at the 3′ end of the DP I cDNA (lower case). This oligo in the antisense orientation was used in a PCR reaction with a sense oligo 5′-GTAGGAAGAATTCCTGC-3′ that was located 70-bp upstream from the end of DP I at an EcoRI site. The EcoRI fragment was subcloned into pl. The full DP.CT was then cut out with a SacI/KpnI digest and blunt end ligated into pRC4B (kindly provided by Dr. R. Scarpulla, Northwestern University, Evanston, IL).

Construction of pDP.ROD. A 35-mer oligonucleotide, 5′-AAGAGCTCGCCATGGagaaagccatcaaggagaag-3′ was used to insert sequence encoding a SacI restriction site followed by a portion of the Kozak consensus sequence for ribosome binding and an ATG start site (both underlined) 5′ of the predicted rod domain (lower case). A 49-mer oligonucleotide, 5′-TTGAGCTCCTACATGAGGCCGAAGAAagcgatagatcctgcaccccgaa-3′ was used to insert sequence encoding a 15-bp fragment of the neuropeptide substance P (underlined), a stop codon and a SacI restriction site 3′ of the predicted end of the rod domain (lower case). These two oligos (the former sense, the latter antisense) were used in a PCR reaction to generate a 2.7-kb SacI fragment which was subcloned into pGEM9Zf(−). An internal 2.4-kb BglII/EcoRI fragment was removed and replaced with the same fragment from DP I cDNA. The flanking PCR-generated portions of the construct were sequenced to ensure that there were no errors in this region because of PCR. The SacI fragment was then subcloned into pRC4B.

Construction pDP.ΔN. A SacI/BglII fragment from pDP.ROD which encoded the start translation site was ligated into a plasmid containing a BglII/EcoRI fragment of DP I cDNA. An EcoRI/KpnI fragment from pDP.CT which encoded the tag and stop codon was subcloned into the previous plasmid. A SacI/KpnI fragment was then subcloned into pRC4B.

Additional Constructs. Expression plasmids were constructed with both tags using a similar approach. In addition, tagless constructs for both pDP.CT and pDP.ΔN were generated using PCR primers not containing the tag sequences.

DNA Transfections

DNA was transfected into COS-7 and NIH-373 cells using the calcium phosphate method (Graham and Van der Eb, 1973) followed by a 15% glycerol shock (Parker and Stark, 1979). Cells were fixed 48 h after glycerol shock unless otherwise noted in the text.

Preparation and Immunoblotting of Whole Cell Extracts

Whole cell extracts were prepared as described by Green et al. (1991). Protein content was determined by the method of Bradford (1976). Samples of 30 μg were loaded and run on SDS-polyacrylamide gels (6.5%). The gels were transferred to nitrocellulose and immunoblotting was performed as previously described (Angst et al., 1990). Primary antibodies used were a 1:2,000 dilution of an affinity-purified rabbit polyclonal, NW 6, directed against a fusion protein of the carboxyl terminus of DP (Angst et al., 1990);

a 1:500 dilution of a mouse monoclonal, DPI-2.17, directed against DP I (Cowin et al., 1985); and a 1:10 dilution of a mouse monoclonal, 9E10.2, directed against an 11 amino acid fragment of human c-*myc* (Evans et al., 1985). Primary antibody binding was detected with a 1:1,000 dilution of peroxidase-coupled anti-rabbit or anti-mouse secondary antibodies (Kirkegaard and Perry Laboratories, Inc., Gaithersburg, MD).

Immunofluorescence Labeling

For immunohistochemistry, cells were grown on glass coverslips. After transfection, cells were washed in PBS and fixed in either methanol (−20°C) for 2 min or 4% paraformaldehyde (25°C) for 10 min. Cells fixed with paraformaldehyde were extensively washed in PBS and were permeabilized by incubation in 0.2% Triton X-100 in PBS on ice for 5 min.

Primary antibodies used for staining were a 1:10 dilution of a mouse monoclonal, 9E10.2 directed against an 11 amino acid fragment of human c-*myc* (Evans et al., 1985); a 1:50 dilution of a rat monoclonal antibody, NCI/34, directed against substance P (Accurate Chem. & Sci. Corp., Westbury, NY); a 1:50 dilution of an affinity-purified rabbit polyclonal antiserum, NW 6, directed against a fusion protein of the carboxyl terminus of DP (Angst et al., 1990); a 1:20 dilution of a mouse mAb directed against DP I and II (Boehringer Mannheim Corp., Indianapolis, IN); a 1:10 dilution of a rat mAb, TromaI, directed against mouse K8 (kindly provided by Dr. K. Trevor and later obtained from the Developmental Studies Hybridoma Bank under control N01-HD-6-2915 from the National Institute of Child Health and Human Development); a 1:5 dilution of a mouse mAb, RGE 53, directed against human K18 (ICN Immunobiologicals, Lisle, IL); a 1:50 dilution of a rabbit polyclonal anti-vimentin antiserum (ICN Immunobiologicals); and a 1:10 dilution of a mouse monoclonal, E7, directed against β-tubulin (Developmental Studies Hybridoma Bank). A 1:10 dilution of rhodamine phalloidin (Molecular Probes, Eugene, OR) was used as a probe for f-actin. All antibodies were diluted in PBS.

To visualize the primary antibody, appropriate fluorescein- or rhodamine-conjugated anti-rabbit, anti-mouse (Kirkegaard and Perry Laboratories), or anti-rat (Jackson ImmunoResearch Laboratories, Inc., West Grove, PA) secondary antibodies were diluted 1:20 in PBS. Controls included incubation of fixed cells in conjugated secondary antibodies alone and with preimmune rabbit serum for polyclonal antibodies.

EM: Conventional and Immunogold Labeling

Transfected COS-7 cells were processed for conventional EM as previously described (Green et al., 1991). For immunogold labeling, cells were grown and transfected on nonetching plastic Permanox tissue culture dishes (Electron Microscopy Sciences, Fort Washington, PA). The cells were fixed overnight in 4% paraformaldehyde plus 0.1% glutaraldehyde in 0.1 M sodium phosphate (pH 7.4). The cells were then washed in cacodylate buffer and dehydrated in a 30, 50, and 70% ethanol series. This was followed by two washes of a mixture of 70% ethanol and LR White resin (Electron Microscopy Sciences) for 1 h each. The cells were infiltrated in LR White for 24 h at room temperature. Fresh LR White was then added and polymerized at 60°C in the presence of nitrogen gas. Sections were placed on nickel grids which were used for immunogold labeling.

Grids were blocked in a 1:20 dilution of normal goat serum in TBS plus 1% BSA (TBS-BSA) for 30 min (all steps at room temperature). Primary antibodies used for staining were a 1:20 dilution of a mouse monoclonal, 9E10.2, and a 1:200 dilution of a mouse monoclonal, V9, directed against vimentin (ICN ImmunoBiologicals). These antibodies were diluted in TBS-BSA and applied to grids for 1 h. The grids were then washed in TBS-BSA plus 0.1% Tween and then were incubated for 1 h with a 15-nm gold-labeled goat anti-mouse antibody (Amersham Corp., Arlington Heights, IL) that was diluted 1:10 in TBS-BSA. The grids were then washed again in TBS-BSA plus 0.1% Tween. In specific experiments noted in the text, grids were counterstained with 3% uranyl acetate for 1 min and lead citrate for 1 min. Controls included incubation without a primary antibody and with the mouse mAb, E7, against β tubulin.

Results

Expression of Mutant DP Domains in COS-7 Cells

cDNA sequences precisely corresponding to the predicted carboxy-terminal globular domain (DP.CT), the central rod domain (DP.ROD), and the carboxyl terminus plus the rod

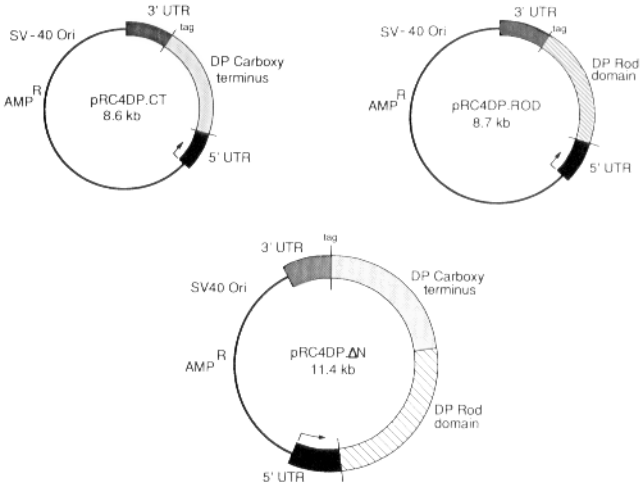

Figure 1. Expression vectors encoding the predicted carboxyl terminus (*pRC4DP.CT*), the predicted rod domain (*pRC4DP.ROD*), and the carboxyl terminus plus the rod domain (*pRC4DP.ΔN*) of DP I. These constructs are referred to in the text as pDP.CT, pDP.ROD, and pDP.ΔN, respectively.

(amino-terminal deletion designated DP.ΔN) (Green et al., 1990) were cloned into the eukaryotic expression vector, pRC4B (Evans and Scarpulla, 1988). This vector uses the rat cytochrome c promoter and intron enhancer sequences to drive the expression of a cDNA insert. In addition, it encodes an SV-40 origin of replication, which increases the copy number of the plasmid in cells such as COS-7 that express large T antigen (Gluzman, 1981), thus further enhancing expression. Domain-specific constructs of DP cDNA were generated by a combination of PCR mutagenesis and routine subcloning techniques. DNA sequence analysis was used to verify structure of the completed constructs (for details see Materials and Methods). Peptide tags encoding either a 5-amino acid fragment of substance P (Albers and Fuchs, 1987, 1989) or an 11-amino acid epitope of c-*myc* (Munro and Pelham, 1987) were used to follow the expression of mutant DP in immunolocalization experiments. Peptide tags were used in part because species-specific DP antibodies were not readily available. Two different tags were used to ensure that observations concerning the effects of each domain were not affected by a specific peptide tag. For simplicity, the constructs in Fig. 1, pRC4DP.CT, pRC4DP.ROD, and pRC4DP.ΔN, will be referred to herein as pDP.CT, pDP.ROD, and pDP.ΔN, respectively.

These constructs were transiently transfected into COS-7 cells by calcium phosphate precipitation and cell extracts were processed 48 h after glycerol shock for analysis by SDS-PAGE. A rabbit polyclonal antibody directed against a fusion protein of the carboxyl terminus of DP used for immunoblotting (Angst et al., 1990) reacted only with the 90 and 185-kD proteins expressed by pDP.CT and pDP.ΔN, respectively, as well as the endogenous 240 and 210-kD DP I and II. (These values reflect relative migration on SDS-PAGE. The actual molecular masses of DP I and II based on the predicted amino acid sequence are 310 and 238 kD, respectively; Virata et al. 1992) (Fig. 2). A DP I-specific mAb, DPI-2.17 (Cowin et al., 1985), which has been epitope mapped to the DP I-specific region of the rod (Nilles, L., and K. Green, unpublished results), reacted with only the 95

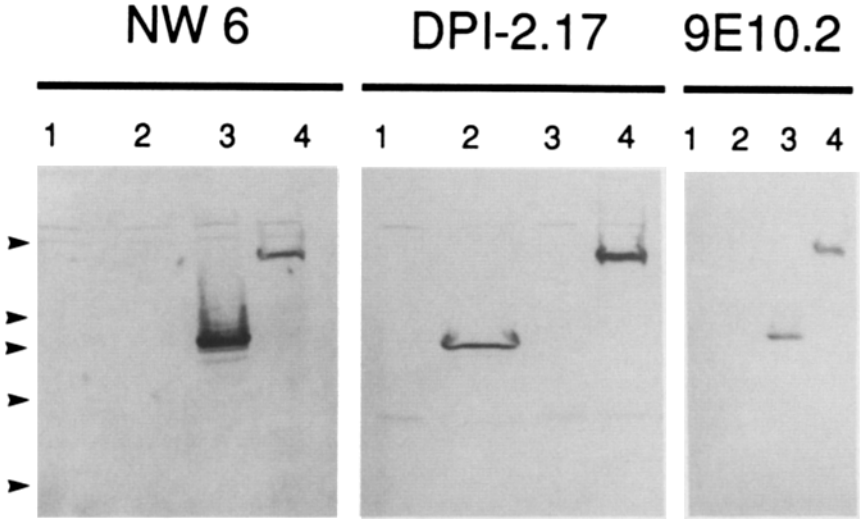

Figure 2. Detection of mutant DP expressed in COS-7 cells by immunoblotting. COS-7 cultures were transfected with each DP construct and were lysed in urea sample buffer at 48 h after glycerol shock. 30 μg of total protein from COS-7 transfected with no DNA (lanes *1*), pDP.ROD (lanes *2*), pDP.CT (lanes *3*), or pDP.ΔN (lanes *4*) were loaded and run on a 6.5% SDS–polyacrylamide gel. These gels were transferred to nitrocellulose and incubated with a rabbit polyclonal antibody directed against the carboxyl terminus of DP (*NW 6*), a mouse monoclonal directed against DP I (*DPI-2.17*) or a mouse monoclonal directed against an 11-amino acid epitope of c-*myc* (*9EI0.2*). The latter antibody recognizes only lanes *3* and *4* as pDP.ROD is tagged with substance P in this experiment. Arrows indicate molecular mass standards of 200, 116.5, 97.4, 66.2, and 42.7 kD, from top to bottom.

and 185-kD proteins expressed by pDP.ROD and pDP.ΔN, respectively, as well as the endogenous DP I. The 9E10.2 mAb directed against an 11-amino acid residue fragment of c-*myc* reacted on immunoblots only with protein expressed by pDP.CT and pDP.ΔN tagged with this epitope (Evans et al., 1985). Antibodies specific for a fragment of substance P reacted only with proteins tagged with this epitope (not shown).

From the immunoblots, the relative amounts of each DP domain expressed appeared to be approximately equal and in each case appeared to be many times higher than endogenous DP (Fig. 2). To make a quantitative estimate on a population basis, transfected cells were metabolically labeled and extracts were immunoprecipitated using a polyclonal antibody to DP I that was reactive to all three mutants (not shown). Taking into account transfection efficiency, the relative amount of protein expressed by each construct was approximately equivalent and was 15–20-fold higher than endogenous DP I as determined by densitometric scanning of autoradiograms.

Immunolocalization of protein expressed from each construct 48 h after glycerol shock demonstrated interesting and

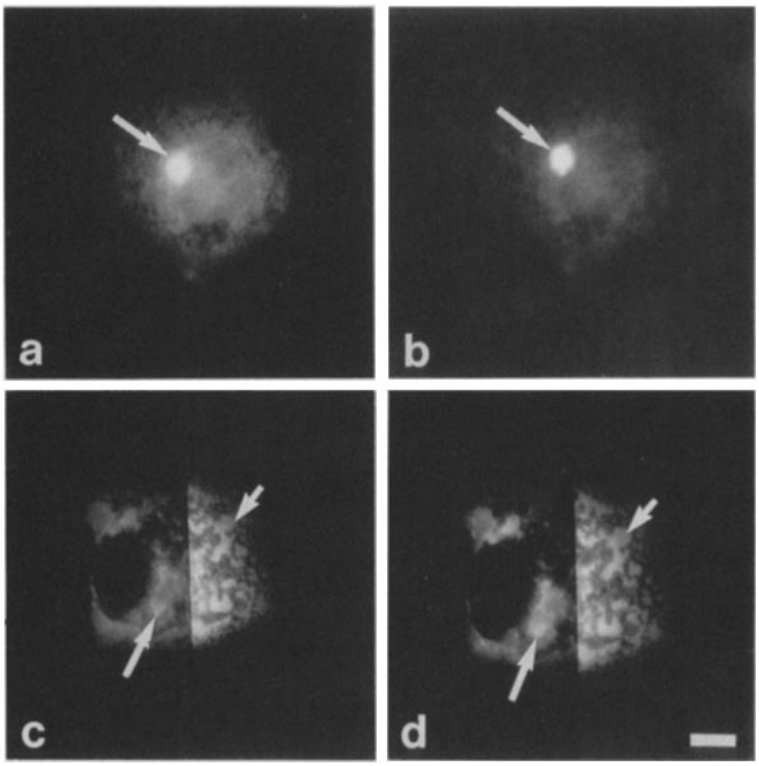

Figure 3. Indirect double label immunofluorescence of COS-7 cells transfected with pDP.CT (*A* and *B*) or pDP.ΔN (*C* and *D*) 48 h after glycerol shock. *A* and *C* were stained with the rabbit polyclonal antibody, NW 6. *B* and *D* were stained with the mouse monoclonal, 9E10.2, which is specific for the c-*myc* tag on transfected mutant DP. Long arrows in all panels identify the perinuclear aggregate. Because of the intensity of this aggregate in *C* and *D*, two different exposures are shown for each panel to clearly demonstrate the cytoplasmic spots (*short arrows*). Bar, 10 μm.

distinct phenotypes. Immunofluorescence analysis using antibodies to DP or to the c-*myc* tag revealed the presence of large perinuclear aggregates as well as diffuse cytoplasmic staining in cells expressing pDP.CT (Fig. 3, *a* and *b*). The expression of pDP.ΔN also resulted in the formation of large perinuclear aggregates as well as an array of discrete spots in the cytoplasm (Fig. 3, *c* and *d*). These cytoplasmic spots appeared to be similar to those formed by the protein expressed by pDP.ROD in transfected cells (see Fig. 5*a*).

Effect of Mutant DP on Cytoskeletal Systems of COS-7 Cells

A series of double-label immunofluorescence experiments were performed to determine if endogenous cytoskeletal systems were affected by the overexpression of these mutant proteins. We were particularly interested in possible effects on IF networks. We observed that COS-7 cells express both type III vimentin and type I and II keratins, although the expression of keratin filaments was decreased in sparse cultures typically used for transfection. This phenomenon has been previously observed with cultured epithelial cells (Rheinwald and O'Connell, 1985). We also observed that COS-7 cells were capable of synthesizing desmosomal components, which is consistent with the epithelial nature of these cells. However, under the culture conditions used for transient transfection, desmosomes were formed only occasionally. Therefore we focused our analysis on the effects of each DP domain on IF.

Double label indirect immunofluorescence of COS-7 cells transfected with either pDP.CT or pDP.ΔN revealed a striking reorganization of both keratin and vimentin networks into tight, often perinuclear, aggregates. Fig. 4, *b* and *d* demonstrates this for pDP.CT and similar results were obtained with pDP.ΔN (not shown). In both cases, the disrupted IF colocalized with the perinuclear aggregate of mutant DP. At this level of expression, >90% of transfected cells had completely disrupted IF, as compared to untransfected COS-7 cells in which 10–15% of the cells were typically observed to have disorganized IF networks. This pattern in untransfected cells is possibly a result of the transient reorganization of IF shown to occur in certain cells during mitosis (Aubin et al., 1980). The disruption was specific for IF as neither the microtubule nor the microfilament systems were affected (Fig. 4, *e–h*). Intriguingly, the perinuclear aggregate colocalized with the microtubule organizing center (Fig. 4, *e* and *f*). IF disruption was also specific for constructs containing the carboxyl terminus of DP, as cells that expressed the rod domain of DP I alone did not have any apparent disruption of vimentin (Fig. 5, *a* and *b*) or keratin (Fig. 5, *c* and *d*) networks. As in untransfected cells, 10–15% of cells transfected with pDP.ROD were observed to have disorganized vimentin networks that did not colocalize with the cytoplasmic aggregates of protein expressed from this vector.

The nature of the carboxy-terminal–induced IF disruption was investigated by examining earlier times after transfection, using the same amount of the expression vector DNA. Mutant DP was first detected by immunofluorescence 9 h after glycerol shock. Protein expressed from both pDP.CT and pDP.ΔN displayed a striking colocalization with intact IF (Fig. 6, *a–d*), while the protein expressed from pDP.ROD was diffuse in the cytoplasm (not shown). Occasional local differences in the DP.CT and vimentin patterns were observed, presumably because of the additional colocalization of mutant protein with the keratin network. These data were obtained using the 9E10.2 antibody to the c-*myc* tag (similar results were obtained with DP antibody), thus confirming that the colocalization was with exogenous mutant DP. At times 9–24 h after glycerol shock, many transfected cells contained bundles of IF that colocalized with mutant DP expressed from either pDP.CT or pDP.ΔN. These IF appeared to be in the process of disruption as by 24 h most were completely disrupted in transfected cells. The result of the time course experiment indicated that the IF disruption was not because of the formation of a mutant protein aggregate which then secondarily caused IF to collapse. Similar colocalization was also observed when the amount of plasmid used in the transfection was decreased by two-thirds and cells were assayed at 24 h after glycerol shock. The colocalization and the disruption of IF were observed with DP carboxyl terminus–containing constructs that were tagless or tagged with either substance P or c-*myc*.

COS-7 cells transfected with pDP.CT and pDP.ΔN were also assayed at 72–144 h after glycerol shock. At these later time points, colonies of transfected COS-7 cells with disrupted IF were observed. By 144 h, the percentage of transfected cells as determined by immunofluorescence was greatly decreased suggesting that the continuous overexpression of these constructs was ultimately toxic to cells. Immunofluorescence of the remaining viable cells expressing mutant DP typically demonstrated either the presence of short IF around the perinuclear aggregate or colocalization of mutant DP with completely reformed IF networks. It is possible that these cells were in the process of recovery and expressed very little, if any, mutant protein.

Examination of Transfected COS-7 Cells by EM

The aggregates of mutant protein and disrupted IF in COS-7 cells transfected with pDP.CT and pDP.ΔN were analyzed in more detail at the ultrastructural level by both conventional and immunogold EM. The perinuclear aggregates observed at the light microscope level in cells transfected with pDP.CT appeared to comprise an electron-dense accumulation of smaller aggregates in the cytoplasm of the cell that were neither located within vesicles nor associated with the nuclear membrane (Fig. 7, *a* and *b*). Immunogold labeling of transfected cells demonstrated that the aggregates contained both mutant DP and vimentin throughout the entire structure (Fig. 7, *c* and *d*), implying that the IF network did not simply collapse around a preformed aggregate of mutant DP. As a control, a mAb to β-tubulin specifically labeled the cytoplasm, but not the aggregates in transfected cells (Fig. 7 *e*).

Mutant protein in cells transfected with pDP.ΔN localized to two distinct types of aggregate (Fig. 8, *a* and *b*). One type of aggregate was similar to the perinuclear aggregates of DP.CT in that it contained both mutant DP protein and vimentin throughout (Fig. 8, *c* and *d*). However, the ultrastructure of the vimentin-containing DP.ΔN aggregates was quite different. While aggregates of DP.CT were electron dense with no apparent filamentous substructure, aggregates of DP.ΔN were composed of a filamentous meshwork. The fine filaments of this meshwork were shorter and of smaller diameter than the 8–10-nm cytoplasmic IF found in neighboring nontransfected cells. The second type of aggregate in

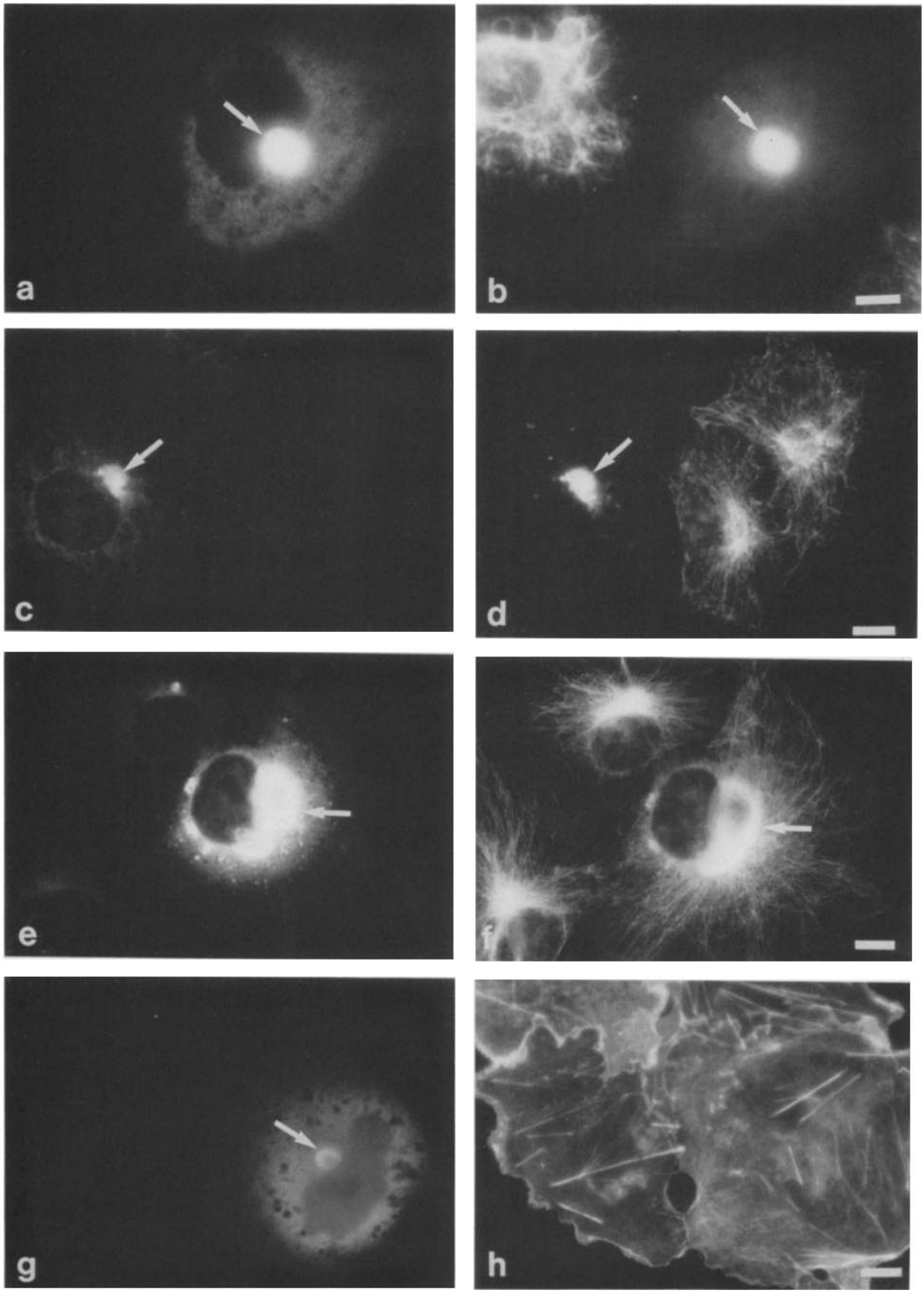
a
b
c
d
e
f
g
h

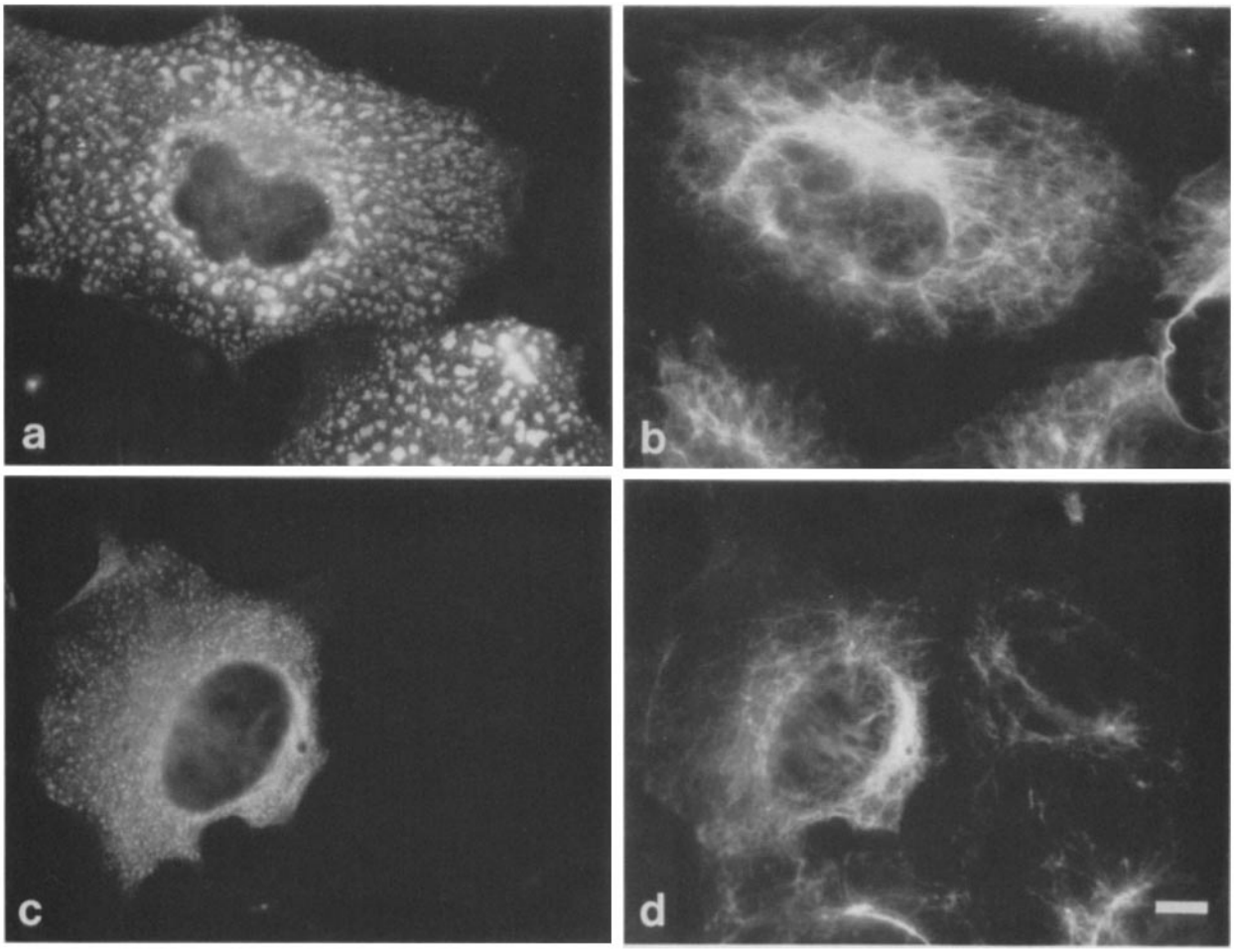

Figure 5. Indirect double label immunofluorescence of COS-7 cells transfected with pDP.ROD tagged with substance P, 48 h after glycerol shock. *a* and *b* were stained with DPI-2.17 and a vimentin polyclonal antibody, respectively. *c* and *d* were stained with a rabbit polyclonal antibody directed against DP and RGE 53, directed against K18. Bar, 10 μm.

cells transfected with pDP.ΔN was electron dense, nonfilamentous, and did not contain vimentin (Fig. 8, *e* and *f*). Their appearance was similar but not identical to the cytoplasmic aggregates observed in cells transfected with pDP.ROD, which also were not labeled by a vimentin mAb (not shown). It should also be noted that an unrelated antibody directed against β-tubulin did not label either type of aggregate, but was restricted primarily to the cytoplasm.

Expression of Mutant DP Domains in NIH-3T3 Cells Resulted In a Similar Pattern of Immunolocalization

It is possible that the apparent association of the carboxyl terminus of DP with IF in COS-7 cells was because of the presence of other desmosomal proteins present in these cells that acted as cofactors or linking proteins. To test this, mutant DP constructs were transiently transfected into NIH-3T3 mouse fibroblasts that do not form desmosomes. In each construct, the patterns of expression observed by double-label indirect immunofluorescence were similar to those seen in COS-7 cells. Immunofluorescence analysis of NIH-3T3 cells transfected with either pDP.CT or pDP.ΔN 48 h after glycerol shock, revealed similar patterns of expression observed at various time points in COS-7 cells. At 48 h after glycerol shock, mutant protein colocalized with intact vimentin networks in certain cells (Fig. 9, *a* and *b*) and disrupted vimentin networks in others (Fig. 9, *c* and *d*). This variable phenotype was likely to be a result of different levels of expression

Figure 4. Indirect double label immunofluorescence of COS-7 cells transfected with pDP.CT (c-*myc* tagged in *a*, *b*, *g*, and *h*, and substance P tagged in *c–f*) 48 h after glycerol shock. *a* and *b* were stained with 9E10.2 and a rabbit polyclonal antibody directed against vimentin, respectively. *c* and *d* were stained with NW 6 and a mouse mAb directed against K18 (RGE 53), respectively. Both the vimentin and keratin networks were collapsed in transfected cells and colocalized with the perinuclear aggregate of mutant DP. *e* and *f* were stained with NW 6 and a mouse mAb directed against β tubulin (E7). *g* and *h* were stained with 9E10.2 and rhodamine phalloidin to label actin filaments. Neither the microtubule nor the microfilament systems were altered in the transfected cells. The results were identical using the c-*myc* or the substance P tag. Arrows indicate the location of the perinuclear aggregate. Bars, 10 μm.

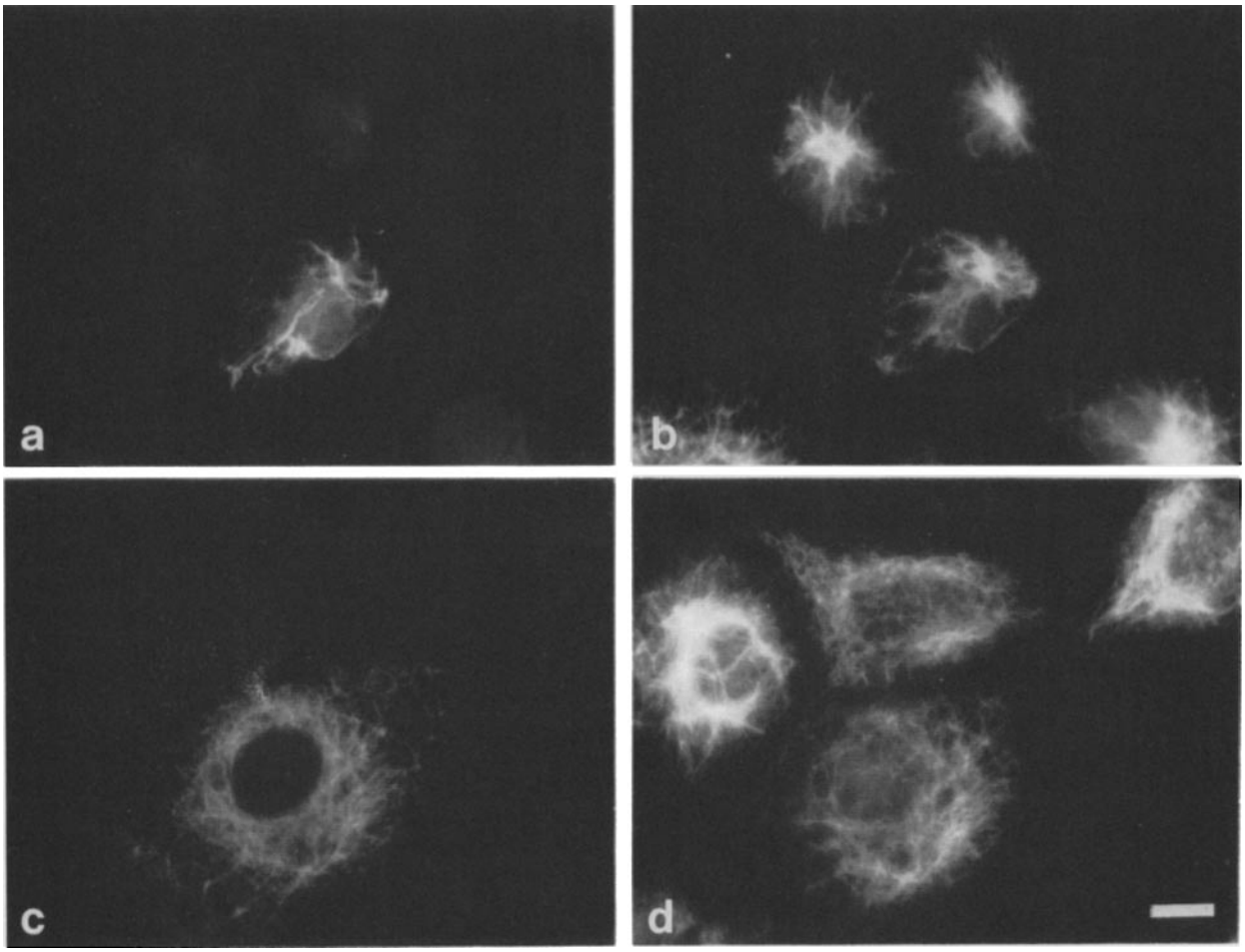

Figure 6. Indirect double label immunofluorescence of COS-7 cells transfected with pDP.CT (*a* and *b*) or pDP.ΔN (*c* and *d*) 9 h after glycerol shock. *a* and *c* were stained with 9E10.2, to identify c-*myc* tagged mutant DP. *b* and *d* were stained with a vimentin polyclonal antibody. At this time point, both mutant DPs colocalize with the vimentin IF system in transfected cells. Bar, 10 μm.

among transfected cells. Both the colocalization and disruption were noted to be more pronounced with DP.ΔN, possibly because of its potential to dimerize. This result implies that proteins restricted to desmosomes may not be absolutely required to either stabilize or mediate the observed association between carboxy-terminal containing mutants of DP and IF.

Discussion

We have presented evidence that truncated DP comprising the predicted carboxyl terminus specifically colocalizes with IF in COS-7 and NIH-3T3 cells. When expressed at high levels, IF networks in these cells are ultimately disrupted. Several lines of evidence suggest that this effect is specific both for the carboxyl terminus of DP and for the IF system. First, the rod domain of DP expressed in either cell line neither colocalized with nor disrupted IF. The possibility that differing levels of expression were responsible for the apparent specificity was ruled out by quantifying levels of mutant DP expression in transfected cells. Second, microtubule and microfilament systems were not obviously affected by the overexpression of any domain of DP. Finally, other investigators have overexpressed the entire keratin 18 cDNA in COS-1 cells using a vector with a strong promoter and an SV-40 origin of replication (Blouin et al., 1990). While K18 incorporated into the endogenous filament network, the "excess" K18 accumulated in a juxtanuclear site similar to the aggregates produced in cells overexpressing DP.CT. However, in cells overexpressing K18, the keratin network remained undisturbed and the vimentin network was only partially reorganized. Therefore overexpression of an insoluble cytoskeletal molecule is not sufficient to disrupt IF even when the molecule can interact normally with endogenous IF at lower levels of expression.

In addition to the disruption of IF observed in cells that overexpressed DP.CT and DP.ΔN, we also observed coalignment without disruption in cells that were most likely expressing lower amounts of these mutant proteins. This evidence argues for the specificity of the interaction. That the effects described above are specific for the IF system is also reflected in the nature of the disruption and the ultrastructure of the resulting aggregates. Electron microscopical analysis revealed that at high levels of expression, IF did not just collapse into whorls around the nucleus, as occurs in response to heat shock (Shyy et al., 1989) or pharmacological agents such as colchicine (for review see Klymkowsky et al., 1989). Instead, IF in transfected cells appeared to disassemble and

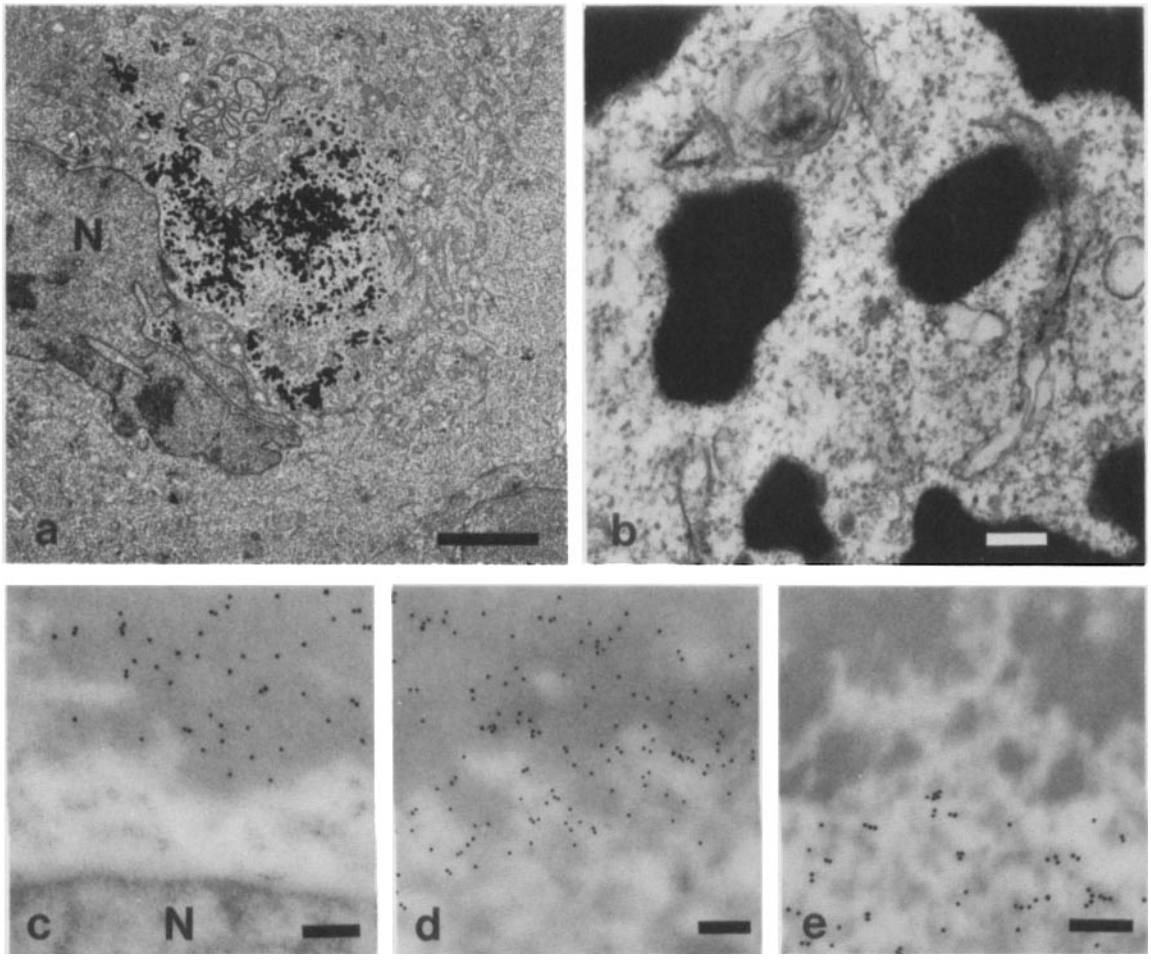

Figure 7. EM of COS-7 cells transfected with pDP.CT 48 h after glycerol shock. Cells were fixed either for conventional EM (*a* and *b*) or for immunogold EM (*c–e*). Clusters of extremely electron-dense aggregates in cells transfected with this construct, at low (*a*) and high (*b*) magnification. Postembedment immunogold labeling of these aggregates was done with the mouse mAbs: 9E10.2, directed against the c-*myc* peptide tag (*c*); V9, directed against vimentin (*d*); and E7, directed against β tubulin (*e*). The gold particles conjugated to anti-mouse secondary antibodies were 15 nm in diameter. Due to the density of these aggregates, the sections were not counterstained. Therefore, the aggregates appear to be less electron dense. The edge of labeled aggregates was shown in the figures to demonstrate the specificity for either the aggregate (*c* and *d*) or for the cytoplasm (*e*). Note that under the conditions of LR White embedment without counterstaining microtubules cannot be visualized even though their antigenicity is retained (*e*). *N*, nucleus. Bars: (*a*) 1 μm; (*b–e*) 0.25 μm.

subsequently, IF subunits became reorganized into electron dense (DP.CT) or fine filamentous meshworks (DP.ΔN) also containing mutant protein. The apparent disassembly we observed is more in line with observations by Klymkowsky (Klymkowsky, 1981; Klymkowsky et al., 1983), in which microinjection of antibodies directed against intermediate filaments resulted in a disappearance of the IF system. IF disruption has also been observed as a result of expressing of dominant negative mutations of keratins (Albers and Fuchs, 1987, 1989; Kulesh et al., 1989; Lu and Lane, 1990; Trevor, 1990) and the 19-kD product of the E1B oncogene (White and Cipriani, 1989, 1990). However, in these latter cases, an ultrastructural analysis of the affected IF networks was not performed. Therefore, we cannot speculate on the potential similarities with the disrupted filaments we observed.

As described above both DP.CT and DP.ΔN were capable of forming aggregates with vimentin. However, as demonstrated by conventional and immunogold EM, the vimentin-containing aggregates were ultrastructurally quite different. Those formed with DP.CT were electron dense and not noticeably filamentous while those formed with DP.ΔN comprised a fine filamentous meshwork. In addition, non-vimentin-containing aggregates of DP.ΔN or DP.ROD did not consist of fine filaments. It follows that to form filamentous aggregates, the rod domain and carboxy-terminal domains of DP as well as vimentin were all necessary. It is possible that the rod domain of DP.ΔN allowed the formation of dimers and/or oligomers that interact with vimentin to create higher order structures whose ultrastructure differed so dramatically from the dense aggregates formed by DP.CT and vimentin. It may be noteworthy that the DP.ΔN-vimentin-containing aggregates ultrastructurally resemble the meshwork of 4–5-nm fine filaments that comprise the innermost desmosomal plaque (Pirbazari and Kelly, 1985). It is possible that by overexpression of this portion of DP which can associate with itself and vimentin, a large plaque-like structure is assembled in the cytoplasm. Expression of full-length DP including the amino terminus may facilitate the localization of this meshwork to the cell cortex.

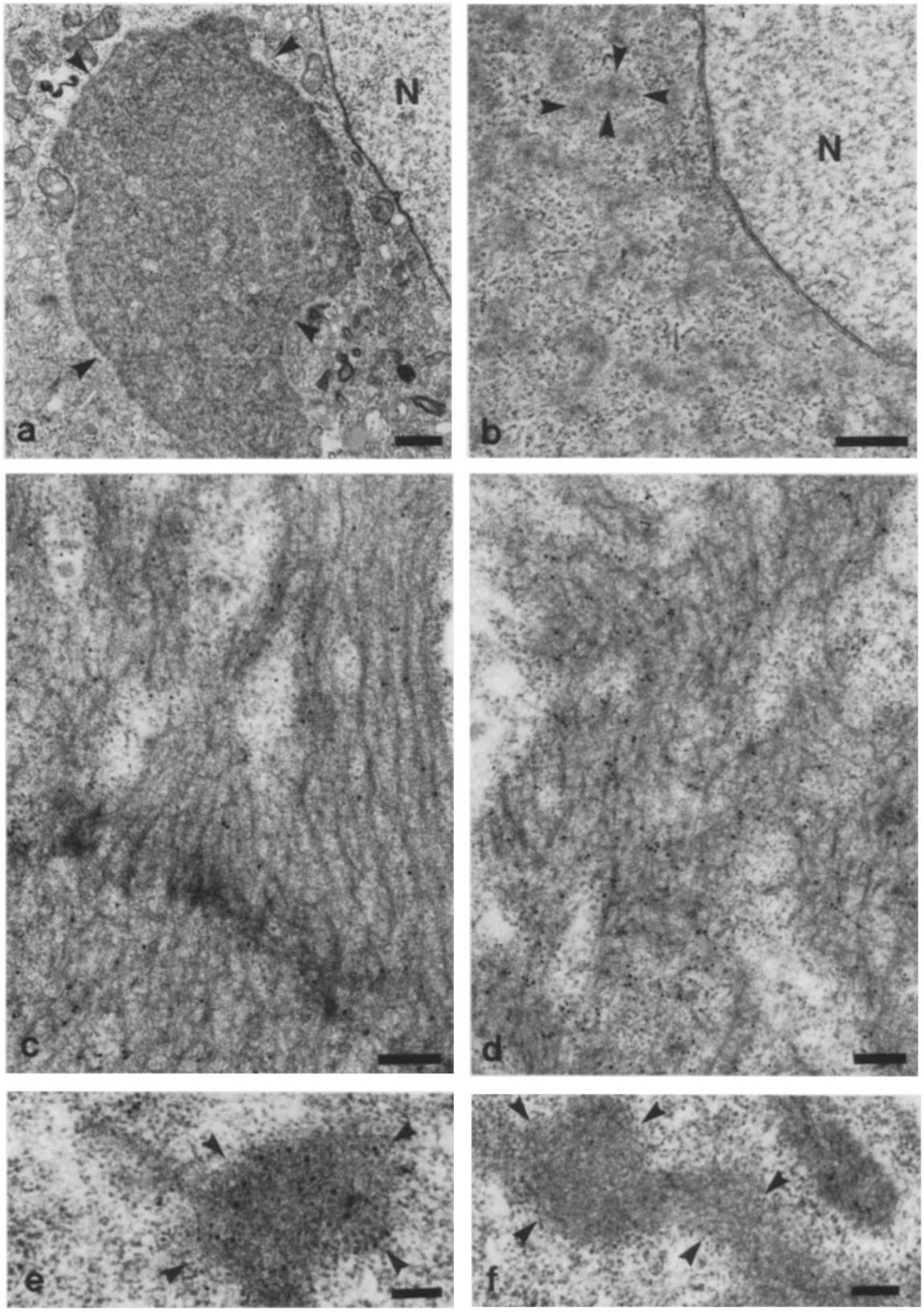

Figure 8. EM of COS-7 cells transfected with pDP.ΔN 48 h after glycerol shock. Cells were fixed either for conventional EM (*a* and *b*) or for immunogold EM (*c–f*). Large filamentous aggregates were observed near the nucleus (N), as shown in *a*, and many smaller, electron-dense spots were seen in the cytoplasm of cells transfected with this construct (as shown in *b*). Postembedment immunogold labeling of transfected cells was carried out with the mouse mAbs: 9E10.2, directed against the c-*myc* peptide tag (*c* and *e*) and, V9, directed against vimentin (*d* and *f*). *c* and *d* are high magnifications of the filamentous perinuclear aggregate that were vimentin positive. *e* and *f* are high magnifications of the cytoplasmic electron-dense spots that were vimentin negative. These sections were counterstained so that the fine filamentous meshwork was visible. Bars: (*a*) 5 μm; (*b*) 1 μm; and (*c–f*) 0.25 μm.

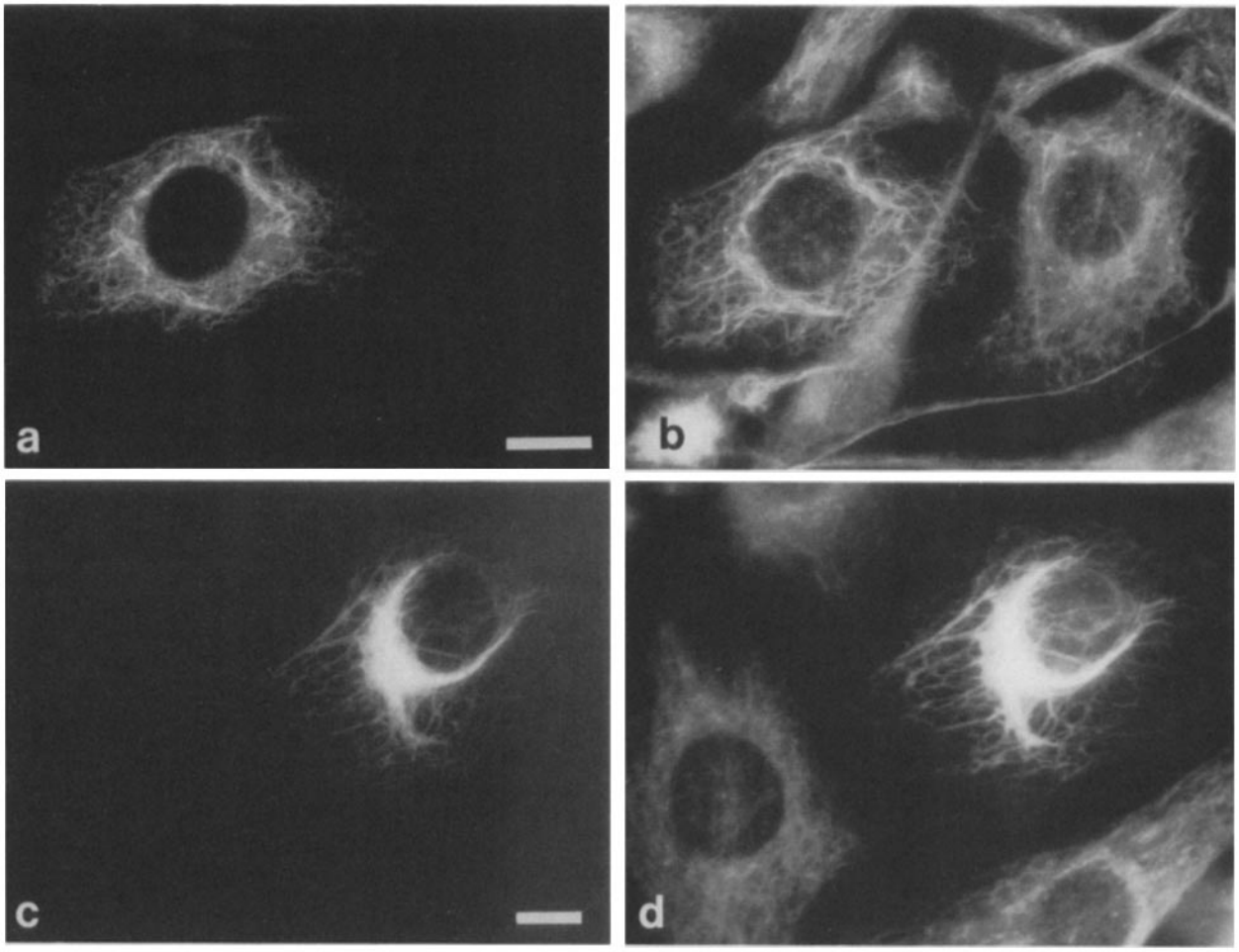

Figure 9. Indirect double label immunofluorescence of NIH-3T3 cells transfected with tagless pDP.ΔN 48 h after glycerol shock. *a* and *c* were stained with DPI-2.17, to identify mutant DP and *b* and *d* were stained with a vimentin polyclonal antibody. In any one population of transiently transfected fibroblasts, a range of phenotypes that appeared to be correlated with the level of mutant expression was observed. The transfected cell (*a* and *b*) in which mutant DP coaligned with vimentin networks, is representative of cells that appeared to express lower levels of DP.ΔN. The transfected cell (*c* and *d*), in which the vimentin network is disrupted and colocalized with mutant-DP staining, is an example of a cell that appeared to express higher levels of DP.ΔN. Bars, 10 μm.

The colocalization of the carboxyl terminus of DP along IF also indicates that this domain of DP may be involved in linking IF to the desmosome. The nature of this linkage still remains to be determined. In vitro binding experiments have so far been unable to demonstrate a direct interaction between DP and IF or any other molecule. One possible explanation for these results, is that the conformation of DP was altered as a result of the denaturing conditions used to solubilize DP during purification, and that this prevented the direct binding of DP to IF. However, it is possible that one or more cellular cofactors or linking proteins may be required to stabilize and/or mediate the association of DP to IF. This would explain the colocalization of DP and IF observed in tissue culture cells when no DP–IF interaction has been reported in vitro. However, the colocalization of the carboxyl terminus of DP with vimentin observed in transfected NIH-3T3 cells makes it unlikely that these factors are other proteins restricted to desmosomes.

Other molecules localized to desmosomes have been demonstrated to bind IF in vitro. However, one of these, DP IV, is only present in desmosomes of stratified epithelia (Kapprell et al., 1988) while others, including desmocalmin (Tsukita and Tsukita, 1985), a 140-kD lamin B related protein (Cartaud et al., 1990), and plectin (Foisner et al., 1991) are present in much smaller amounts than DP in the desmosome. DP IV, desmocalmin, and the 140-kD lamin B related protein are likely to be restricted to desmosomes and therefore, in light of the 3T3 results, are unlikely to be absolutely required for a DP–IF association. This does not exclude the possibility that they play some sort of stabilizing role in the plaque of the desmosome, thus explaining previous in vitro binding data. Certain desmosomal molecules, such as plectin, are not restricted to desmosomes and are also located in mesenchymal tissues. Therefore we cannot rule out that the DP–IF interaction observed in fibroblasts is not stabilized or mediated by such a protein.

The coalignment of DP.CT along IF may have implications for the normal process of desmosome assembly. Although it is not clear if intact IF networks are needed for desmosome formation, previous investigators have suggested that DP is translocated to the cell surface in association with IF during the formation of desmosomes (Jones and Goldman, 1985; Pasdar and Nelson, 1988). In these experiments desmosome assembly was induced in cultured epithelial cells by switch-

ing cells from low to normal calcium, at which time DPs appeared to become redistributed from the cytoplasm to the cell surface. During the early stages of assembly, DP-containing spots formed a discontinuous linear pattern along IF. Ultimately these spots were cleared from the cytoplasm and DP became restricted to cell–cell interfaces. The colocalization of the carboxyl terminus of DP with IF during transient transfection may be mimicking the process by which endogenous DP are assembled into desmosomes. One possible explanation for the continuous pattern of DP.CT and DP.ΔN along IF is that the increased level of expression saturated sites of IF association. Consistent with this idea is that in cases where lower levels of protein appear to be expressed, a more discontinuous, dotty pattern can be observed (Fig. 9*a*). Because COS-7 cells form only a small number of immature desmosomes as determined by EM, it has been difficult to determine the effect of the expression of any portion of DP on desmosome formation in these cells. We are currently transfecting individual DP domains into cell lines that have a greater number of mature desmosomes to study incorporation and/or disruption of desmosomes.

We wish to thank Dr. Michael Klymkowsky for providing 9E10.2 antibody, Dr. Katrina Trevor for providing Troma I antibody, Dr. Pamela Cowin for providing DPI-2.17 antibody, Dr. Elaine Fuchs for providing substance P antibody, and Dr. Richard Scarpulla for providing pRC4B. We would also like to express our appreciation to Liza Virata, M. Kathleen Rundell, Jonathan Jones, Eileen White, and Rex Chisholm for helpful discussions and Hue Luu for excellent technical assistance. Special thanks go to Walter Glogowski for technical expertise in preparing specimens for EM.

This work was supported in large part by National Institutes of Health (NIH) grant HD24430, and aided by a March of Dimes Basic Research grant 1-FY91-0140 and an American Cancer Society Junior Faculty Research Award to K. J. Green. Additional support was provided by grant No. 2432 from the Council for Tobacco Research, USA, Inc. T. Stappenbeck was supported in part by NIH training grant T32-GM08061.

Received for publication 23 September 1991 and in revised form 9 December 1991.

References

Albers, K., and E. Fuchs. 1987. The expression of mutant epidermal keratin cDNAs transfected in simple epithelial and squamous cell carcinoma lines. *J. Cell Biol.* 105:791–806.

Albers, K., and E. Fuchs. 1989. Expression of mutant keratin cDNAs in epithelial cells reveals possible mechanisms for initiation and assembly of intermediate filaments. *J. Cell Biol.* 108:1477–1493.

Angst, B. D., L. A. Nilles, and K. J. Green. 1990. Desmoplakin II expression is not restricted to stratified epithelia. *J. Cell Sci.* 97:247–257.

Arnn, J., and L. A. Staehelin. 1981. The structure and function of spot desmosomes. *Dermatology.* 20:330–339.

Aubin, J. E., M. Osborn, W. W. Franke, and K. Weber. 1980. Intermediate filaments of the vimentin type are distributed differently during mitosis. *Exp. Cell Res.* 129:149–165.

Blouin, R., H. Kawahara, S. French, and N. Marceau. 1990. Selective accumulation of IF proteins at a focal juxtanuclear site in COS-1 cells transfected with mouse keratin 18 cDNA. *Exp. Cell Res.* 187:234–242.

Bradford, M. M. 1976. A rapid and sensitive method for the quantitation of microgram quantities of protein utilizing the principle of protein-dye binding. *Anal. Biochem.* 72:254–259.

Cartaud, A., M. A. Ludosky, J. C. Courvalin, and J. Cartaud. 1990. A protein antigenically related to nuclear lamin B mediates the association of intermediate filaments with desmosomes. *J. Cell Biol.* 111:581–588.

Conway, J. F., and D. A. D. Parry. 1990. Structural features in the heptad substructure and longer range repeats of two-stranded α-fibrous proteins. *Int. J. Biol. Macromol.* 12:328–334.

Cowin, P., H-P. Kapprell, and W. W. Franke. 1985. The complement of desmosomal plaque proteins in different cell types. *J. Cell Biol.* 101:1442–1454.

Evans, G. I., G. K. Lewis, G. Ramsey, and J. M. Bishop. 1985. Isolation of monoclonal antibodies specific for human *c-myc* proto-oncogene product. *Mol. Cell. Biol.* 5:3610–3616.

Evans, M. J., and R. C. Scarpulla. 1988. Both upstream and intron elements are required for elevated expression of rat somatic cytochrome c gene expression in COS-1 cells. *Mol. Cell. Biol.* 8:35–41.

Foisner, R., B. Feldman, L. Sander, and G. Wiche. 1991. Monoclonal antibody mapping of structural and functional plectin epitopes. *J. Cell Biol.* 112: 397–405.

Garrod, D. R., E. P. Parrish, D. L. Mattey, J. E. Marston, H. R. Measures, and M. J. Vilela. 1990. Desmosomes. *In* Morphoregulatory Molecules. G. M. Edelman, B. A. Cunningham, and J. P. Thiery, editors. John Wiley & Sons Inc., New York. 315–339.

Gluzman, Y. 1981. SV-40 transformed simian cells support the replication of early SV-40 mutants. *Cell.* 23:175–182.

Graham, F. L., and E. Van der Eb. 1973. A new technique for the assay of infectivity of human adenovirus 5 DNA. *Virology.* 52:456–467.

Green, K. J., and J. C. R. Jones. 1990. Interaction of intermediate filaments with the cell surface. *In* Cellular and Molecular Biology of Intermediate Filaments. R. D. Goldman and P. M. Steinert, editors. Plenum Publishing Corp., New York. 147–174.

Green, K. J., D. A. D. Parry, P. M. Steinert, M. L. A. Virata, R. M. Wagner, B. D. Angst, and L. A. Nilles. 1990. Structure of the human desmoplakins: implications for function in the desmosomal plaque. *J. Biol. Chem.* 265:2603–2612.

Green, K. J., T. S. Stappenbeck, S. Noguchi, R. Oyasu, and L. A. Nilles. 1991. Desmoplakin expression and distribution in cultured rat bladder epithelial cells of varying tumorigenic potential. *Exp. Cell Res.* 193:134–143.

Jones, J. C. R., and R. D. Goldman. 1985. Intermediate filaments and the initiation of desmosome assembly. *J. Cell Biol.* 101:506–517.

Kapprell, H-P., P. Cowin, W. W. Franke, and H. Ponsting. 1985. Biochemical characterization of desmosomal proteins isolated from bovine muzzle epidermis: amino acid and carbohydrate composition. *Eur. J. Cell Biol.* 36:217–229.

Kapprell, H-P., K. Owaribe, and W. W. Franke. 1988. Identification of a basic protein of M_r 75,000 as an accessory desmosomal plaque protein in stratified and complex epithelia. *J. Cell Biol.* 106:1679–1691.

Kelly, D. E. 1966. Fine structure of desmosomes, hemidesmosomes, and an adepidermal globular layer in developing newt epidermis. *J. Cell Biol.* 28:51–72.

Klymkowsky, M. W. 1981. Intermediate filaments in 3T3 cells collapse after the intracellular injection of a monoclonal anti-intermediate filament antibody. *Nature (Lond.).* 291:249–251.

Klymkowsky, M. W., R. H. Miller, and E. B. Lane. 1983. Morphology, behavior, and interaction of cultured epithelial cells after antibody-induced disruption of keratin filament organization. *J. Cell Biol.* 96:494–509.

Klymkowsky, M. W., J. B. Bachant, and A. Domingo. 1989. Functions of intermediate filaments. *Cell Motil. Cytoskeleton.* 14:309–331.

Kozak, M. 1986. Point mutations define a sequence flanking the AUG codon that modulates translation by eukaryotic ribosomes. *Cell.* 44:283–292.

Kulesh, D. A., G. Cecena, Y. M. Darmon, M. Vasseur, and R. G. Oshima. 1989. Posttranslational regulation of keratins: degradation of mouse and human keratins 18 and 8. *Mol. Cell Biol.* 9:1553–1565.

Lu, X., and E. B. Lane. 1990. Retrovirus-mediated transgenic keratin expression in cultured fibroblasts: specific domain functions in keratin stabilization and filament formation. *Cell.* 62:681–696.

Mueller, H., and W. W. Franke. 1983. Biochemical and immunological characterization of desmoplakins I and II, the major polypeptides of the desmosomal plaque. *J. Mol. Biol.* 163:647–671.

Munro, S., and H. R. B. Pelham. 1987. A C-terminal signal prevents secretion of luminal ER proteins. *Cell.* 48:899–907.

O'Keefe, E. J., H. P. Erickson, and V. Bennett. 1989. Desmoplakin I and desmoplakin II: purification and characterization. *J. Biol Chem.* 264:8310–8318.

Parker, B. A., and G. R. Stark. 1979. Regulation of simian virus 40 transcription: sensitive analysis of the RNA species present early in infections by virus or viral DNA. *J. Virol.* 31:360–369.

Pasdar, M., and W. J. Nelson. 1988. Kinetics of desmosomal assembly in Madin-Darby canine kidney epithelial cells: temporal and spatial regulation of desmoplakin organization and stabilization upon cell–cell contact. II. Morphological analysis. *J. Cell Biol.* 106:687–695.

Pasdar, M., K. A. Krzeminski, and W. J. Nelson. 1991. Regulation of desmosome assembly in MDCK cells: coordination of membrane core and cytoplasmic plaque domain assembly at the plasma membrane. *J. Cell Biol.* 113:645–655.

Pirbazari, M., and D. E. Kelly. 1985. Analysis of desmosomal intramembrane particle populations and cytoskeletal elements: detergent extraction and freeze-fracture. *Cell Tissue Res.* 241:341–351.

Rheinwald, J. G., and T. M. O'Connell. 1985. Intermediate filament proteins as distinguishing markers of cell type and differentiated state in cultured human urinary tract epithelia. *Ann. NY Acad. Sci.* 455:259–267.

Schwarz, M. A., K. Owaribe, J. Kartenbeck, and W. W. Franke. 1990. Desmosomes and hemidesmosomes: constitutive molecular components. *Annu. Rev. Cell Biol.* 6:461–491.

Shyy, T. T., B. B. Asch, and H. L. Asch. 1989. Concurrent collapse of keratin filaments, aggregation of organelles, and inhibition of protein synthesis during heat shock response in mammary epithelial cells. *J. Cell Biol.* 108: 997–1008.

Steinberg, M. S., H. Shida, G. J. Guidice, M. Shida, N. H. Patel, and O. W.

Blaschuk. 1987. On the molecular organization, diversity and functions of desmosomal proteins. *In* Junctional Complexes of Epithelial Cells. G. Bock and S. Clark, editors. John Wiley & Sons Inc., New York. 3–43.

Steinert, P. M., and D. R. Roop. 1988. Molecular and cellular biology of intermediate filaments. *Ann. Rev. Biochem.* 57:593–625.

Tanaka, T., D. A. D. Parry, V. Klaus-Kovtun, P. M. Steinert, and J. R. Stanley. 1991. Comparison of molecularly cloned bullous pemphigoid antigen to desmoplakin I confirms that they define a new family of cell adhesion junction plaque proteins. *J. Biol. Chem.* 266:12555–12559.

Trevor, K. T. 1990. Disruption of keratin filaments in embryonic epithelial cell types. *New Biol.* 2:1004–1014.

Tsukita, S., and S. Tsukita. 1985. Desmocalmin: a calmodulin-binding high molecular weight protein isolated from desmosomes. *J. Cell Biol.* 101: 2070–2080.

Vasser, R., P. A. Coulombe, L. Degenstein, K. Albers, and E. Fuchs. 1991. Mutant keratin expression in transgenic mice causes marked abnormalities resembling a human genetic skin disease. *Cell.* 64:365–380.

Virata, M. L. A., R. M. Wagner, D. A. D. Parry, and K. J. Green. 1992. Molecular structure of the human desmoplakin I and II amino terminus. *Proc. Natl. Acad. Sci. USA.* 89:544–548.

White, E., and R. Cipriani. 1989. Specific disruption of intermediate filaments and the nuclear lamina by the 19-kDa product of the adenovirus E1B oncogene. *Proc. Natl. Acad. Sci. USA.* 86:9886–9890.

White, E., and R. Cipriani. 1990. Role of adenovirus E1B proteins in transformation: altered organization of intermediate filaments in transformed cells that express the 19-kilodalton protein. *Mol. Cell Biol.* 10:120–130.

Wiche, G., B. Becker, K. Luber, G. Weitzer, M. J. Castanon, R. Hauptmann, C. Stratowa, and M. Stewart. 1991. Cloning and sequencing of rat plectin indicates a 466-kD polypeptide chain with a three-domain structure based on a central alpha helical coiled coil. *J. Cell Biol.* 114:83–99.